AE-47

An experimental study of the scattering of slow neutrons from H_2O and D_2O.

Karl-Erik Larsson, Sten Holmryd and Kåre Otnes

AKTIEBOLAGET ATOMENERGI

STOCKHOLM · SWEDEN · 1960

AN EXPERIMENTAL STUDY OF THE SCATTERING OF SLOW NEUTRONS FROM H_2O AND D_2O.

Karl-Erik Larsson, Sten Holmryd and Kåre Otnes

Abstract:

The cold neutron technique has been applied to the study of the scattering properties of light and heavy water. It is shown that with respect to neutron scattering water behaves much like a solid. It is estimated that a water molecule occupies a stationary position for a period of $\sim 2 \cdot 10^{-12}$ seconds performing about 10 vibrations before it makes a diffusion jump of a length of at least 1.5 Å. The consequences of the observations for neutron thermalization problems are discussed briefly.

Printed December 1960.

An experimental study of the scattering of slow neutrons from H_2O and D_2O.

1. Introduction.

Until recently the atomic or molecular motions in liquids have been experimentally studied only indirectly. It has been possible to draw conclusions concerning the microscopic fluctuations or the atomic motions just from macroscopic measurements of magnitudes like specific heat, density variations with temperature etc. The X-ray spectroscopy has delivered information of fundamental importance for the understanding of the structure of liquids. From such measurements it has been possible to show that a certain degree of order exists in a liquid, such that at a given instant an atom is surrounded first by a layer of nearest neighbours at a distance of 2 - 4 Å, then by a more diffuse layer of next nearest neighbours etc. These correlations between pairs, however, disappear rather quickly in contrast to what happens in solids. The fact that there is a certain degree of local order in a liquid, would make it reasonable to suppose that the dynamic properties of a liquid would be more like those of a solid than like those of an ideal gas. It would seem reasonable to suppose that a given atom at any instant stands under the influence of the forces from 10 to 20 neighbour atoms. From the experimental results of infrared and Raman spectroscopy conclusions have been drawn not only dealing with the internal motions in a molecule but also with the motion of the molecules relative to each other in certain liquids, water being one of them. So far no experiments have been made from which it should have been possible to decide conclusively, which of the current models would best have described the experimental observation. In this respect the neutron offers a unique possibility and particularly the very slow or cold neutron. Light water, H_2O, happens to be a very suitable liquid for neutron studies because practically all (95 %) scattering from H_2O is incoherent - a typical case of spin incoherence - while the reverse is true for D_2O (~ 80 % coherent cross section). For light water all the atomic motions are displayed in a scattering experiment while for heavy water relative intensity displacements over the spectrum might occur because of the coherence complications. However, both light and heavy water have

a particular interest as they are currently used as reactor moderators. The present work will deal mainly with scattering from H_2O and briefly describe results on the scattering from D_2O.

2. The neutron method.

In the investigation of the atomic dynamics of many body systems like a solid, the neutron occupies a unique position as a probe particle because of its large mass. This fact was clearly pointed out by van Hove[1] and has later been experimentally used in the study of single phonons and of dispersion relations or in the determination of the frequency spectrum of the heat vibrations in solids [2, 3]. Neutrons have also been used to measure the mean life time of phonons in the high frequency region, $\omega \sim 10^{13}$ sec^{-1}, in aluminium[4]. A few cases have been reported, where the powerful neutron method has been used to study atomic motions in liquids for instance in H_2O [5, 6, 7]. The slow neutrons are subject to many interactions with matter of which the inelastic scattering process is the most important one in this connection. The cross section for this scattering reaches appreciable values only when the laws of energy and momentum are fullfilled:

$$E_{out} - E_{in} = \hbar\omega \text{ (Energy gain)} \tag{1}$$

$$\underline{k}_{out} - \underline{k}_{in} = \underline{q} + \underline{\tau} \tag{2}$$

Here $E = \frac{\hbar^2 k^2}{2m} = \hbar\omega$, where $\underline{k}$ is the neutron wave vector; m is the neutron mass, $\underline{q}$ is the phonon wave vector and $\underline{\tau}$ is a vector of the reciprocal lattice. Equation (1) is the energy conservation law, while eq. (2) expresses the coherence conditions. This last equation may, however, formally be looked upon as a true momentum condition. As this equation expresses the coherence condition, it is not valid for the case of incoherent scattering. For coherent scattering the scattered intensity reaches maxima when eq. (1) and (2) are fullfilled simultaneously. If $\omega = q = 0$ and $k_{out} = k_{in}$ we have elastic scattering.

The reason that the neutron is such an excellent probe particle for the study of atomic motions in solids and liquids may be understood in a variety of ways. One may just point towards the fact that the time it takes for a neutron of about one Ångstrom wave length, i.e. with an energy of ~ 0.025 eV, to move a distance of about one Ångstrom, i.e. about the mean atomic or molecular distance in solids or liquids is $\tau \sim \frac{10^{-8}}{10^{5}} = 10^{-13}$ sec. It is also well known that the Debye temperatures of solids fall in the region of a few hundred degrees Kelvin, i.e. the vibration frequency in the short wave length region is of the order $\frac{1}{\omega_D} \sim 10^{-13}$ sec. The slow neutron may thus be said to study the vibrational phenomena on the correct time scale.

It may also be of value to point out the difference between one neutron of wave length < 1 Å, and another of wave length > 4 Å. To make this difference clear, let us make use of the uncertainty relation in the form $\Delta p \, \Delta x \geq \hbar$, The region, Δx, within which the neutron observes a phenomenon decreases with increasing momentum transfer Δp, where Δp is given by eq. (2), $\Delta p = \hbar \cdot \left| \underline{k}_{out} - \underline{k}_{in} \right|$. For a given energy transfer and a given angle of observation, Δx will increase for decreasing k_{in}, i.e. for increasing neutron wave length. If we are studying a body, within which the atoms move with average velocities v, the neutron will be observing an atom at least during a time interval $\delta t = \frac{\Delta x}{v}$. If we, for example, are observing elasticly scattered neutrons of 4 Å wave length at an angle of observation of 30°, we find $\delta t \geq 2 \cdot 10^{-13}$ sec, where the assumption is made that $v = 5 \cdot 10^{4}$ cm/sec. For a 1 Å neutron the corresponding time interval will be $\delta t \geq 6 \cdot 10^{-14}$ sec. The faster the neutron, the shorter is the interaction time. This conclusion seems trivial but, in fact, gives the fundamental reason why a cold neutron is the ideal probe particle. This may be understood, if we study what happens in a solid or liquid as seen from a distinct time t = 0. For very small t, say $t < 10^{-14}$ sec, a molecule or an atom will appear to move approximately with constant speed as a free particle. For times of the order of $t \geq 10^{-13}$ sec., i.e. times of the order of $\frac{1}{\omega_D}$, the free motion is hindered by the action of neighbours. To complete the imaginary picture let us assume that at times of the order of $\geq 10^{-12}$ sec. the atom makes a large instantaneous diffusion jump. From this picture we may see that a super thermal neutron

$E \gtrsim 0.1$ eV, $\lambda \lesssim 1$ Å tends to see an atom as free, while a cold neutron of small energy, $E \sim 0.005$ eV, $\lambda \sim 4$ Å, feels the bond of the atom or molecule because it makes its observation during a time within which the force action is appreciable. The cold neutrons also on the average observe the diffusion jump supposed to happen, but only as a larger uncertainty factor in the definition of the atomic position, i.e. a line broadening would be observed.

A very slow neutron, $E \sim 5 \cdot 10^{-5}$ eV, $\lambda \sim 40$ Å, performing its observation during a time interval $\delta t > 10^{-12}$ sec. would see a complete chaos of atoms making diffusion jumps. The neutron line sent into the diffusing body would be scattered as a very broad line, which would have lost all its sharpness.

The imaginary example just discussed is supposed to serve a dual purpose: a. to illustrate the usefulness of the cold neutron technique for the purpose to study atomic motions on a time scale between 10^{-13} and 10^{-12} sec. and b. to illuminate a model for water, which has been discussed in detail of experimenters [5] as well as theoreticians [8].

3. Experimental technique and results for H_2O.

The experimental filter and time-of-flight technique as well as a detailed analysis of the apparatus used at the Stockholm reactor, R1, to study scattered neutron spectra have been given in great detail elsewhere [9]. Two important facts concerning the technique will once more be stressed:

1. The beryllium filtered spectrum used to send into the sample has a sharp edge at 3.95 Å. The total instrumental resolution used is 30 - 50 μsec/m. in the sense that over a flight path of slightly more than three meters the width of the beryllium cut off is 100 - 160 μsec depending upon the chopper speed used.

2. The spectra scattered or transmitted from the samples may be recorded within an angular range from 0° to 90°. With slight changes, angles up to 130° may be used for observation.

As will soon be shown the interesting part of the spectra scattered from water samples ranged over a wide wave length region from 0.5 to 5 Å. With a flight path of 3 meters this means that observations had to be made within a time interval from 0.4 to 4.5 msec. Because the highest possible resolution was required, an electronic channel width of 30 μsec was the maximum permissible. With a maximum number of 100 channels this meant that two series of observations had to be made to cover the interesting 4 msec interval. Usually one run was made at a chopper speed of 8600 rpm covering a time interval from 1.1 to 4.1 msec and another run made at a chopper speed of 12000 rpm covering a time interval from 0.4 to 3.4 msec. This technique of collecting data gives a wide overlap region from 1.1 to 3.4 msec of great usefulness for the control of the corrections necessary to make. As discussed in detail elsewhere [9] the chopper has a wave length dependent transmission, $T(\lambda, \omega)$. The data thus have to be divided by $T(\lambda, \omega)$ with the proper ω-value inserted. In the wave length regions of interest in the present experiment, this correction never exceeded 20 %. As found from the wide overlap region, this correction is very well known, causing a negligible uncertainty in the intensity values. Another important wave length dependent correction is the correction for the detector efficiency. The detector consists of three layers, containing 10, 9 and 10 counters respectively, each counter consisting of a 30 mm copper tube, 0.5 mm thick, and filled with enriched $B^{10}F_3$ (93 % B^{10}) to a pressure of 600 mm. This compounded detector is not black but has an efficiency, which decreases with decreasing neutron wave length. To transform the results to an intensity scale independent of neutron wave length the values corrected for the chopper function have to be multiplied by a factor increasing with decreasing wave length. This correction term in the actual case, if given a relative value of 1.0 at 4 Å, has a value of 1.12 at 3 Å, 1.42 at 2 Å, 2.40 at 1 Å and 3.22 at 0.7 Å. A great care has been exercised to calculate this correction, consideration being taken not only to the self screening effect to the gas itself, but also to all the surrounding copper shells. The relative uncertainty in this correction factor should not reach a value exceeding a few percent, if compared at 1 and 5 Å. Before any of these corrections may be applied, the background must be substracted from the data. Careful background runs were always made with empty sample holder. The background never exceeded 10 % and must be regarded as a very safe correction.

To avoid an appreciable multiple scattering in a water (H_2O) sample, this must be thin having a thickness of the order of 0.2 mm to give a transmission of 90 % or more. Our sample holder was constructed of two thick aluminium plates with a central region, 8 x 9 cm^2, milled down to a thickness of 1 mm. The distance between the plates was defined by an aluminium ring placed outside the O-rings, which made the sample space tight. Via a plastic tube entering the lower part of the sample holder the sample space proper was connected to a container with distilled water. The water level was controlled in another plastic tube leaving the top of the sample space. In order to control that the sample space was actually filled without bubble formation even at the smallest sample thickness used, the sample was emptied, then filled again and the measurement repeated. As the intensity stayed constant the conclusion was drawn that the sample was properly filled. In those cases when the sample was heated a resistance band was wired around the insulated edge of the holder and the entire holder was surrounded by a larger aluminium container to avoid air currents causing undesired temperature variations. All parts of the holder, except the thin sample area were covered by 1 mm Cd.

As measurements on samples as thin as 0.2 mm are extremely slow because of the very low intensity scattered, a series of measurements were performed at room temperature with a sample thickness of 1,4 mm H_2O, the spectrum scattered at angles of φ = 30, 50, 70, 90 and 122° being observed to get some general idea about the spectrum shape and its angular variations (fig. 1). These runs - although somewhat distorted by multiple scattering - gives an idea of the complicated nature of the spectrum scattered inelastically as well as elastically. The broad energy gain spectrum ranging from ~ 0.12 eV down to 0.005 eV, shows peaks at 0.063, 0.024, 0.014 and 0.010 eV. A large intensity maximum is also observed at the ingoing energies corresponding to elastic scattering with a reproduction of the ingoing spectrum. A mere glance at the scattering picture shows tendencies well known from the scattering from solids: the intensity of the elastic spectrum decreases with increasing angle of observation, φ, while the intensity of the inelastic spectrum increases with angle, φ. Unfortunately, it is not possible to draw any far reaching conclusions from these observations

before effects of multiple scattering have been investigated in detail. Thus multiple scattering in this case causes the abnormal appearance of the peak at 0.063 eV, which for this sample thickness showed an intensity independent of angle a behaviour which is by no means true for a thin sample as will soon be shown.

To study the effect of sample thickness in detail a number of runs were made with a sample thickness of 5, 2.5, 1.2, 0.5 and 0.2 mm at an angle of observation of $\varphi = 30^{\circ}$ (fig. 2). At very large sample thickness one would of course expect the scattered spectrum to approach the shape of the Maxwell spectrum. In fact, at the largest sample thickness used - 5 mm - the elastic part of the spectrum tends to be destroyed by multiple scattering, the intensity distribution round the peak at 900 μsec gradually approaching the shape of a Maxwellian peak[10]. If the ratio (R) between the intensity scattered at 0.9 msec (1.17 Å) and that scattered at 3.2 msec (4.1 Å) is plotted as a function of sample thickness, figure 3, it is clearly seen that this ratio flattens out to reach a constant or only very slowly varying value for a sample thickness smaller than 0.2 mm. This is taken as a proof that 0.2 mm is a sufficiently small sample thickness to be considered as "thin". This was the basic sample thickness used in the further investigation.

In fig. 4 are given two spectra observed at $\varphi = 30^{\circ}$ and 90° and at a sample thickness of 0.2 mm. These spectra show the same characteristic features as the ones observed at larger thickness: a series rather sharply developed peaks at E = 0.063, 0.024, 0.014 and 0.010 eV. If an energy of 0.004 eV is used as an average ingoing energy this corresponds to observed energy transfers of 0.059, 0.020, 0.010 and 0.006 eV. It is, however, to be observed that the broad ingoing spectrum may strongly distort the scattered spectrum at the position of the small energy transfers of 0.006 and 0.010 eV. Even at 0.020 eV the width of the incoming spectrum may play some role. Only at the position of the highest energy transfer, 0.059 eV, the scattered spectrum is practically uninfluenced of the shape of the cold primary spectrum which is given by $I(\lambda) \sim \lambda^{-5}$ from $\lambda = 3.95$ Å[10]. The intensity of the inelasticly scattered spectrum varies strongly with angle φ in such a way, that for a given energy transfer the intensity increases with increasing momentum transfer, $\underline{k}_{out} - \underline{k}_{in} = \underline{\kappa}$.

The elasticly scattered spectrum shows a sharp edge at the position of the Be cut off, 3.96 Å. The intensity of the elastic peak varies in a direction opposite of the inelastic peaks: it decreases with increasing momentum transfer. In the immediate neighbourhood of the elastic peak and partly mixed up with it, an increase in the scattered intensity is observed which might possibly be identified as small inelasticly scattered peaks of which one could occur at 0.0058 eV and another at 0.0045 eV. These possible, small energy transfers of $\pm$ 0.0006 eV are not visible at $\varphi = 30^{\circ}$, but already at $\varphi = 50^{\circ}$ the intensity has increased so that both peaks are visible. The intensity then increases with increasing angle, φ. From now on the elasticly and the inelasticly scattered intensity regions will be treated separately.

The elastic or quasi-elastic scattering

The fundamental separation of the observed spectra into one elastic part, curve IV, and one inelastic part, curves I + II + III, is given in fig. 5. The reason for this particular separation will be made clear during the course of the analysis. To start the discussion, let us accept this separation as a first approximation. If the quasi-elastic part is drawn separately, curves are obtained, which may be compared to the primary spectrum of neutrons. This has been done in fig. 6, where the runs at $\varphi = 30^{\circ}$ and 90° are compared to the primary spectrum, which was determined in two ways:
1. it was measured directly in straight transmission at $\varphi = 0^{\circ}$, and
2. it was measured by scattering from a vanadium sample. When the latter spectrum was corrected for absorption in the sample, it very closely agreed with the one measured in straight transmission. The two spectra are given with the observed relative intensities. In these two spectra as well as in those observed at other angles, two main effects are visible:

1. The intensity of the spectrum decreases with increasing momentum transfer, κ.
2. A small but resolved broadening of the sharp beryllium cut off at 3.96 Å occurs. This is most easily seen at an angle φ of 30°.

In addition to these main effects there are the possible, small energy transfers of $\pm$ 0.0006 eV mentioned above and visible in fig. 6. These make the 90° observation angle one of the most inconvenient angles, if one wants to study line broadening. A detailed analysis of these two spectra as well as others taken at other angles and sample thicknesses give identical results as to relative intensity variation and line broadening.

The experimentally observed width of the beryllium cut off, Δt_{obs}, is found to fall between the limits 210 and 270 μsec for the different angles, φ, between 30° and 122°. The resolution width, Δt_r, determined from the vanadium scattered spectrum is 160 $\pm$ 5 μsec as observed at a chopper speed of 8600 rpm. A considerable line broadening is thus observed. The natural line width, Δt_n, is calculated from the formula

$$\Delta t_n = \sqrt{(\Delta t)^2_{obs} - (\Delta t)^2_r}$$

The result of the analysis is given in fig. 7. *) The natural line widths are found to fall within a band shown in the figure:

$$\Delta E \approx (6 \pm 1) \cdot 10^{-4} \text{ eV}.$$

There might be a slight tendency of increase of the width with increasing angle of observation or increasing momentum transfer $\varkappa$. For comparison, two theoretical line widths are given in the figure. As any broadening of the elastic peak should be caused by an uncertainty in the atomic position or a diffusion of the atoms or molecules the predictions of these two models are chosen because they correspond to two extreme models for this process. In one of the models it is anticipated that the molecules perform a continuous diffusion [11]. The line width is then described by the relation

$$\Delta E = 2 \hbar D \varkappa^2 \qquad (3)$$

*) Note added in proof: The assumption that the line has a Gaussian shape might cause some systematic error in the line width value. Also we have later found that if it is assumed that the true line shape is Lorenzian, the width read from the slope of the edge of the beryllium cut off is about 35 % too large. Therefore there might be a systematic error in the value of the width given above in such a way that ΔE should be decreased to about 4×10^{-4} eV. The shape of the curve of figure 7 is however not changed. A similar reasoning holds for the data of figure 10.

i.e. a linear dependence of κ^2. D is the self diffusion constant. As shown by the figure this hypothesis is in sharp contrast to experiment. The other model [8] assumes that the molecules perform a number of vibrations around an instantaneous equilibriumposition for a time τ_o and then make a relatively large diffusion jump for a time τ_1 and so on. In one extreme case one may let $\tau_1 \longrightarrow 0$ when the line width is given by

$$\Delta E = \frac{2\hbar}{\tau_o} \left(1 - \frac{e^{-2W}}{1 + \kappa^2 D \tau_o} \right) \qquad (4)$$

in the other extreme case, when $\tau_o \longrightarrow 0$, the formula (3) describes the width. In fig. 7 the line width is calculated according to (4) with $\tau_o = 2 \cdot 10^{-12}$ sec and with $2W = 0.142\ \kappa^2$ (compare the text below). The value of D is taken as $1.85 \cdot 10^{-5}$ cm^2/sec. As will be seen this calculated line width agrees much better with experiment. It seems, however, that the experimentally observed widths stay more constant as a function of κ^2 than what is predicted from formula (4). The value of τ_o is given with a precision of ~ 25 %: $\tau_o = (2 \pm 0.5) \cdot 10^{-12}$ sec. Combinations of different values of τ_o and τ_1 do not give any better fit to experiment. The conclusion that may be drawn at this stage of the investigation is that a molecule vibrates round an equilibrium position for a time of ~ $2 \cdot 10^{-12}$ sec and then makes an instantaneous large diffusion jump to another "lattice" site.

As clearly shown by fig. 6 the intensity of the elastic peak decreases strongly with angle, φ. Experimentally the intensity may be defined in several ways. We have used two different methods to measure it. In one case the value of the intensity is read at the position of the beryllium cut off 3.95 Å. This intensity value, called $I_{1/2}$, is then multiplied by the half value width ΔE given above to correspond to an integral J over a small region round 3.95 Å. In the other case the observed intensities according to curve IV are summed over a number of channels corresponding to the width value, i.e. of the order of ten channels of 30 μsec each. In fact it was found that the two methods of determining the intensity variation gave similar results. In fig. 8 $J = I_{1/2} \cdot \Delta E$ determined according to the first

method is given on a semi logaritmic plot as a function of κ^2. As will be seen J is very well described by a function $e^{-u^2\kappa^2}$, where u^2 has the value of $0.142(\text{Å})^2$. The experiment thus shows that the intensity of the elastic peak varies in a manner similar to that scattered from a solid, for which the intensity is given by the Debye-Waller factor $e^{-2W} = e^{-u^2\kappa^2}$. The quasi-crystalline model mentioned above predicts an intensity variation of the type e^{-2W}. According to the continuous diffusion model the intensity of the peak should essentially stay constant and independent of angle as the product $(\frac{d^2\sigma}{d\Omega d\omega})_{\omega=0} \cdot \Delta E$ is independent of κ^2. The experiment thus again seems to verify the model resembling liquid water to a solid. From the value of the constant u^2 one may compute the extension, u, of "thermal cloud" within which the molecule vibrates. This gives 0.38 A in good agreement with measurements of angular distributions at other neutron energies[5]. From u^2 a value of the fictitious Debye temperature of water may be derived, the result being $\theta_D = 130\ ^\circ\text{K}$. The experiment then permits the interpretation that the thermal cloud is well developed, before the molecule makes a diffusion jump. The average length, ℓ, of this jump may be computed from the random walk formula

$$\ell^2 \sim 6\, D\, (\tau_o + \tau_1) \qquad (5)$$

With $D \sim 2 \cdot 10^{-5}$ cm^2/sec, $\tau_o = 2 \cdot 10^{-12}$ sec and $\tau_1 = 0$ the answer is $\ell \sim 1.5$ Å. This value has to be considered as a lower limit, as it is not possible to give any value of τ_1 from this experiment.

Another important check of the quasi-crystalline model of water is to study the intensity variation of the elastic as well as the inelastic scattering with sample temperature. With a sample thickness of 0.5 mm we therefore made a number of observations of the scattered spectrum at $\varphi = 30^\circ$ and for sample temperatures of T = 22, 40, 60, 77 and 92 $^\circ$C. A few examples of the results are given in fig. 9. If we here limit ourselves to the observations of the elastic peak we find that the sharp beryllium cut off at 3.96 Å (3.1 msec) is increasingly broadened with increasing temperature. Also the peak intensity drops with increasing temperature. The result of an analysis of the line widths is given in fig. 10. The natu-

ral width increases from about 5 to $7.5 \cdot 10^{-4}$ eV, i.e. with some 50 % from 22 to 92 °C. The increase is, within our limits of error, linear. For comparison the line width variation expected on the basis of the continuous diffusion model mentioned above is also shown in the figure. The theoretical curve is calculated using values of D determined by the spin lattice relaxation method[12]. As seen from the figure the calculated temperature increase of the line width is about four times faster than the experimentally observed when this model is used. It is impossible to compare the experimental result to the prediction of the quasi-crystalline model as the variation of τ_o (and τ_1) with temperature is unknown.

The intensities round 3.95 Å at the different temperatures were evaluated as described above as the product $I_{1/2} \cdot \Delta\Xi = J$. As seen from fig. 11 J is within our limits of error constant and independent of temperature. The dotted line corresponds to the calculated variation from $e^{-2W} = e^{-a^2T}$ with a^2 determined from the value of $\theta_D = 130$ °K. The other model - corresponding to the idea of continuous diffusion - predicts an intensity independent of temperature. It is thus impossible to decide between the models from the present experiment, the result being in agreement with both models. An observation at $\varphi = 90^\circ$ could have been better, but there the small inelasticly scattered peak at 0.0058 eV complicates interpretation.

Finally it should be repeated once again that there are possibly some very small energy transfers corresponding to an energy gain and loss of about $(5 - 7) \cdot 10^{-4}$ eV. It is, however, impossible with the present technique to make any closer analysis of these "peaks" for several reasons. One of these is, that it is impossible to tell exactly how curve III (fig. 5) should be extrapolated in under curve IV. Another obvious reason is that the broad primary spectrum severely distorts the shape of these "peaks." A third reason is that even if the beryllium filter transmits a spectrum with a sharp edge at 3.96 Å there also is a small intensity at 3.58 A. A fourth reason is that - even if it is a small effect - there is a minor contribution from coherent scattering which might distort the elastic peak slightly, particularly so at $\varphi = 90^\circ$ (compare the measurements on

D_2O described below).

Inelastic scattering.

As already discussed a broad spectrum of inelasticly scattered neutrons ranging from ~0.12 eV down to the primary energy of 0.005 eV is observed. The data essentially making the basis for the following discussion are already shown in figures 4 and 9, where fig. 4 shows the correct angular variation (thin sample, 0.2 mm) and fig. 9 shows the important features of the temperature variation of the spectrum (0.5 mm sample).

With a spectrum of this kind and with the knowledge that a quasi-crystalline model fairly well describes the elastic scattering, it would seem logic to assume the entire inelastic spectrum to be a result of an irreducible frequency spectrum similar to the one observed in vanadium [3]. As is well known such a spectrum - if present - entirely determines the scattering cross section $\frac{d^2\sigma}{d\Omega dE}$ in the incoherent approximation [13]. The spectrum, $g(\omega)$, might then be calculated from a formula

$$g(\omega) \sim \frac{k_o}{k} \cdot \frac{\omega}{\kappa^2} \cdot \frac{e^{\frac{\hbar\omega}{k_B T}} - 1}{e^{-u^2\kappa^2}} \cdot I_{obs} \qquad (6)$$

where $\hbar\omega$ is the energy transfer corresponding to the momentum transfer $\underline{\kappa} = \underline{k} - \underline{k}_o$. I_{obs} is the observed intensity proportional to the differential cross section and assumed to be corrected for the multi-phonon terms, which are of great importance if $T \geq \theta_D$. A spectrum of a similar kind is observed in hydrides like zirconium hydride and copper hydride [14, 15]. In the actual case this spectrum would then have a strong peak at 0.059 eV corresponding to a longitudinal optical vibration and a weaker one at 0.020 eV corresponding to a transverse optical vibration. The energy transfers at 0.014 and 0.010 eV should then correspond to two groups of acoustic

vibrations of longitudinal and transverse nature respectively. A rough theoretical estimate of the ratio between the longitudinal optical and the longitudinal acoustic vibration frequencies gives the ratio $\omega_{opt}/\omega_{ac.} \sim 4$. As the neutron flight time t corresponding to a vibration frequency ω is determined by $\omega \sim t^{-2}$, the ratio between the corresponding flight times would be $\frac{t_{opt}}{t_{ac}} \sim \frac{1}{2}$. In the spectrum observed the optical peak should be the one at t = 0.9 msec. corresponding to 0.063 eV, why the acoustic longitudinal peak should fall at a flight time of about 1.8 msec. As an inspection of the figures 1, 2, 4 and 9 shows this amazingly well corresponds to the peak observed at 0.014 eV.

This interpretation of the spectrum, however, encounters with difficulties. With a frequency spectrum of the anticipated type, the Debye temperature should be higher than the observed value, $\theta_D = 130\ ^oK$. It could, however, be possible that the vibrations of the H atoms contribute very little to θ_D. Further the interaction between the molecules would be so strong that the identity of the molecules were lost, the O and H atoms vibrating freely as in a diatomic lattice.

In the place of the interpretation of the inelasticly scattered spectrum just discussed, another one would be possible. This has already been proposed, at least partly, by the observations in infrared and Raman spectroscopy [16, 17]. According to this model the intense peak at 0.063 eV should correspond to a hindered rotation of the molecule. The transition in the region of 0.024 eV should correspond to a particular type of vibration where the four corner molecules of a tetrahedron should vibrate against the molecule situated in the centre of the tetrahedron. The rest of the spectrum could then very well consist of an acoustic vibrational spectrum with the molecule as a dynamic unit. This division of the inelastic spectrum is already illustrated in fig. 5. This interpretation gets a strong support from two facts:

1. The Deby temperature, 130 ^oK, found from the intensity variation of the elastic peak corresponds to an energy transition of $\sim$ 0.011 eV in good agreement with the observed peak at 0.010 eV.

2. If the inelastic cross section in the Debye approximation [13] is calculated for $\varphi = 30$ and 90°, including one, two and three phonon terms and the result integrated over the entire energy scale the ratio between the integrals $(\frac{d\sigma}{d\Omega})_{90^{\circ}} / (\frac{d\sigma}{d\Omega})_{30^{\circ}}$ is found to be 2.60. If on the other hand the ratio between the areas under the experimental curves III taken at 90° and 30° is calculated it is found to be 2.70. The angular variation of $\frac{d\sigma}{d\Omega}$ taken over this part of the inelastic spectrum is thus well described by a Debye model with $\theta_D = 130\ ^{\circ}K$. The corresponding curves are given in fig. 12.

As is also shown by this figure the shape of the spectrum is not correctly predicted by a Debye spectrum. The observed spectrum shows two intensity maxima in better agreement with the hypothesis of an acoustic longitudinal and an acoustic transverse intensity maximum. It should be emphasized that the extrapolation of curve III in under the elastic peak is rather uncertain. There is no reason to expect an agreement with a Debye spectrum for the smallest energy transfers. The agreement mentioned above may be interpreted so, that H_2O might very well show an irreducible acoustic frequency spectrum which may be calculated from formula (6). Because of the width of the primary spectrum and the relative smallness of the energy transfers, it seems useless to try a derivation of the shape of this spectrum. However, the facts underlying these ideas, seem to give a strong support to the interpretation already given to the observations on the elastic peak: our probe particle - the neutron - measuring the atomic events on a time scale with a unit of 10^{-13} sec. observes water as a quasi-crystalline structure.

In contrast to these attempts to explain the neutron scattering from H_2O on the basis of a crystalline model, it is of interest to compare to the gas model. Because of its attractive simplicity this model has often been used in connection with spectrum calculations in reactors. It has then been assumed that the water molecules with mass = 18 scatter as free gas atoms. It is to be observed that the cross section calculated on the basis of this model includes all types of scattering, elastic as well as inelastic [13]. In fig. 13 the calculated spectrum for $\varphi = 90^{\circ}$ based on the gas model with

m = 18 is compared to that part of the observed spectrum which could reasonably be so, i.e. the hindered rotation and the vibration at 0.020 eV are excluded. The theoretical curves are normalized to give the same intergrated area $\frac{d\sigma}{d\Omega}$, as the experimental one. As shown by the figure there is no similarity between the theoretical and the experimental curve. To further show the complete disagreement, the average energy $\bar{E}$, of the scattered neutrons is calculated for the two spectra. It is found that the mass 18 curve gives $\bar{E}$ = 0.013 eV while the experimentally observed value is $\bar{E}$ = 0.0055 eV. If the gas model is used with mass 100 - also shown in fig. 13 - this spectrum gives a value for $\bar{E}$ of 0.0059 eV in better agreement with experiment. At smaller as well as larger angles even the mass 100 model gives values of $\bar{E}$ in disagreement with experiment. On an average, however, mass 100 gives a much better agreement with experiment than mass 18. For high neutron energies it is known that mass 1 gives a good result: the proton may be considered as free. It thus seems reasonable to imagine a varying "effective mass" as a scattering centre, increasing with decreasing neutron energy.

For the interpretation of the atomic or molecular motions in H_2O as observed in the present work the gas model is of no value. The experiments shows that for these short time events $\sim 10^{-13}$ sec - water shows strong similarities to a solid structure.

For the calculation of thermalization properties of water and of the final thermal neutron equilibrium spectrum, a crystalline model could very well be used. Observations like those exemplified in figures 4 and 5 could be used to calculate a real or fictitious frequency spectrum. With this spectrum known, the differential cross section formulas already developed for the case of a solid [13] could be used to treat the scattering properties of water. Another way based on the different nature of internal molecular motions and the intra molecular motions has already been used in such computations [18, 19].

4. Results for D_2O

In one respect D_2O is the extreme opposite of H_2O: heavy water scatters slow neutrons almost completely coherently (80 %). A very pronounced effect of this coherence is to be expected particularly in the elastic scattering of the 4 - 5 A neutrons at larger angles, $\varphi > 85^\circ$. This expected effect is most clearly demonstrated by an auxiliary measurement of the angular distribution of the elasticly scattered neutrons using a crystal spectrometer. Such an instrument being in operation at the Stockholm reactor was used to measure this angular distribution. 1.1 A neutrons were sent into a 2 mm thick sample of D_2O. The scattered neutrons were energy analyzed by a second crystal set to select the same wave length as the one sent into the sample, so that to a very good approximation only elasticly scattered neutrons were recorded. The angular distribution obtained in this way is given in fig. 14. This strongly peaked distribution is to be compared with the corresponding angular distribution for H_2O (figure 8) described by the factor $e^{-0.142\,\kappa^2}$. Knowing the distribution according to fig. 14, it is easy to predict what will happen to the elasticly scattered intensity using the cold neutron spectrum as the primary spectrum. The intensity of elasticly scattered neutrons will always be very high for momentum transfers $\kappa = \frac{4\pi}{\lambda_o} \sin \frac{\varphi}{2}$ in the region round 2 $Å^{-1}$ as the angular distribution is peaked at that value. At 90° angle of observation this peak corresponds to 4.4 Å wave length ($\sim$ 3.4 msec in our time-of-flight scale), i.e. it occurs in the middle of the cold spectrum, which will consequently be strongly scattered. At 30° angle of observation the contribution of coherence should be small as 4 Å neutrons are then scattered at $\kappa \sim 0.8\ Å^{-1}$. Here most of the scattering is incoherent.

To investigate the spectrum scattered from D_2O two complete runs were made, one at $\varphi = 90^\circ$ and another at $\varphi = 30^\circ$, with a sample thickness of 2.0 mm, which in this case is a thin sample (transmission 90 %). The result is shown in fig. 15. The spectrum scattered from heavy water thus is very similar to the one observed in light water: there is a broad inelastic spectrum which ranges from 0.1 eV down to 0.005 eV showing one pronounced peak at E = 0.052 eV - corresponding to a transition of 0.048 eV -

and some smaller not resolved "peaks" at about 0.020, 0,013 and 0,010 eV. The top part of the spectrum, ranging from 0,7 to 1.9 msec - appears contracted compared to the corresponding part of the spectrum scattered from H_2O. The part of the inelastic spectrum ranging from 1.9 msec and up towards 3 msec is in the 30° run very similar to the corresponding spectrum scattered from H_2O, while at 90° there is a strong increase in the intensity in this region as compared to the scattering picture for H_2O. This increase very well might be caused by the coherence. On the whole the discussion carried through for the inelasticly scattered spectrum from H_2O might be directly taken over in the case of D_2O.

The real great difference between the scattering from heavy and light water is demonstrated in the elastic part of the scattering. In contrast to the H_2O case, the elastic scattering from D_2O is more intense for 90° then for 30°, the reason being the intense coherent scattering at 90° as explained above. This mixture of coherent and incoherent scattering makes it impossible to derive a Debye temperature for D_2O. A study of the inelastic spectrum with its break structure at E = 0.013 or 0.014 eV and 0.009 or 0.010 eV makes it reasonable to assume about the same Debye temperature of 130 °K, with an uncertainty of some 15 %. Theoreticly, if there should be an acoustic vibrational spectrum, there are no really strong reasons to believe that the intermolecular forces should be radically different in D_2O from those in H_2O. Also the mass difference is so small that the maximum vibrational energy should be about the same also for this reason. It is interesting to note that also in the case of D_2O there is a broadening of the sharp edge at 3.95 Å as compared to the resolution width. The observed width at 30° as well as at 90° falls in the same range as for H_2O, $\Delta t_{obs} \sim 250$ μsec, corresponding to a residence time for a D_2O molecule of about $2 \cdot 10^{12}$ sec before it makes a diffusion jump. Another detail also seems to be repeated in the scattering picture produced by D_2O: at 90° there certainly is some scattered intensity near the beryllium cut off corresponding to an energy transfer of about $6 \cdot 10^{-4}$ eV. In this case it is not possible to observe an energy loss "peak" at 0.0052 - 0.0006 eV which was possible at $\varphi = 90°$ in the case of water (fig. 6).

In conclusion one might say that the neutron spectrum scattered from D_2O reveals the same type of dynamical behaviour of the D_2O-molecules as for the H_2O molecules in liquid water. The differences in the inelastic scattering may well be explained by the coherent scattering. The difference in angular variation of the "acoustic", inelasticly scattered spectrum for $E < 0.014$ eV might very well originate from the same cause. A real difference occures for the scattered peaks at 0.052 and 0.020 eV, which appear at much lower energies than in H_2O. The scattered spectra does not show any similarities to the one calculated from a gas model but may rather be explained on the basis of a quasi-crystalline model.

5. Comparison to other data

Investigations of the dynamical properties of water by use of slow neutrons have been carried out first by Brockhouse [5, 6] and then later by Hughes et al. [7]. While Brockhouse uses a crystal spectrometer to produce the monochromatic neutron beam to be sent into the sample and a crystal as well as time-of-flight technique to analyse the scattered spectrum, the Brookhaven group uses the Be filter technique combined with time-of-flight analysis of the scattered neutron spectrum. The main features of the results gained by the two groups of experimenters are in agreement with the present results:

a. a quasi elasticly scattered peak is observed.
b. an inelasticly scattered spectrum ranging over a wide region of energies is also registered.

The closer interpretation of data in the two cases differs however considerably. As discussed in section II it is to be expected that only very slow neutrons are able to show all the details of the dynamical picture. The use of neutrons of 1 - 2 Å wave length as probe particles requires a very high resolution and consequently a very high neutron flux to resolve all the finer details. Because of this fact it is easy to see why a mass 18 gas model could be said to fit the inelasticly scattered neutron spectrum observed by Brockhouse[5]. As shown by the present experiment as well

as by the Brookhaven data the inelasticly scattered spectrum does not show any similarity to the mass 18 gas model spectrum. On the other hand the angular distribution of elasticly scattered neutrons observed by Brockhouse is in very good agreement with the present data leading to the value of the extension, u, of the thermal cloud of 0.38 Å, where Brockhouse gives 0.4 Å. As to the interpretation of the observed shape and width of the quasi elasticly scattered peak the present results have extended and confirmed the Brookhaven results and are in disagreement with the interpretation of the Brockhouse data [6]. It is our belief that the resolution of the Brockhouse experiment using rotating crystal has not been good enough to resolv the small peaks which we as well as the Brookhaven group observe near the incoming energy at $\pm$ 0.0006 eV on each side of it. As indicated by figure 6, these peaks are not visible at $\varphi = 30^{\circ}$, $\kappa = 0.82$ Å^{-1}, but clearly visible at $\varphi = 90^{\circ}$, $\kappa = 2.24$ Å^{-1}. In fact they are visible already at $\varphi = 50^{\circ}$. If these peaks had not been resolved we would have observed a line width variation in somewhat better agreement with that predicted by the continuous diffusion model and also with that obtained by Brockhouse [6]. It might be argued that the small peaks of figure 6 are not clearly resolved and their origin is unknown. The energy gain peak at 0.0058 eV is not well resolved but the energy loss peak at 0.0046 eV is rather well so. Also the complete set of runs including data taken at $\varphi = 50^{\circ}$ and 70° clearly shows this inelasticly scattered intensity growing while the top part of the beryllium cut off very nearly shows a constant slope independent of these peaks. In the present experiment the resolution $\delta\lambda/\lambda$ was about 5 % at 4 Å. Considering the fact that the intensity of the small subsidiary peaks is small - of the order of 10 % of the intensity in the main quasi-elasticly scattered peak - and the fact that a wave length resolution of better than 3 % should be necessary to see the three peaks completely resolved, it is clear that only a very long running time even at a high flux reactor would be sufficient in order that the peaks appear resolved when a crystal is used to produce a nearly monochromatic neutron beam to be sent into the thin water sample. Our observations as well as our interpretation of data are thus in complete agreement with the results of the Brookhaven group on this point.

The difference between our observations and the Brookhaven results is that because of our somewhat higher resolution (usually $\frac{\delta t}{t} = 3$ % at 4 Å) we are able to see the slight broadening of the quasi-elasticly scattered line at 3.95 Å (compare figures 6 and 7). As, however, the width of the Brookhaven beryllium cut off must be about 200 - 225 μsec (which may be guessed from the fact that a broadening of $0.3 \cdot 10^{-3}$ eV would have been detected) their resolution, $\frac{\delta t}{t} \sim 5$ % at 4 Å, should have been good enough to observe the broadening we observe. The reason why this was not the case is not clear.

Comparing the shape of our complete spectrum observed at 90° and the corresponding spectrum observed at Brookhaven, it is obvious that the ratio between the intensities in the peaks at 0.063 eV to that at 0.0052 eV in the Brookhaven case is about 2 while in our case this ratio is about 1 (figure 4). Only at larger sample thicknesses our spectrum shape approaches that of the Brookhaven group. In fact there are three corrections to be applied to the directly observed data as discussed in section III:

1. Background
2. Chopper transmission function
3. Detector efficiency

As discussed in section III the two first corrections are very safe and reasonably small in our case, while the third is a large, wave length dependent one. We are, however, confident that the possible errors in this correction factor can not exceed 10 %. A factor of two is out of question, so the cause for the discrepancy between our spectrum shape and that observed at Brookhaven is unknown. With the exception of this difference in relative intensity distribution and the difference in observed line broadening, the spectra observed by us and by the Brookhaven group show the same energy transfers and general features.

6. Summary and conclusions

By studying the neutron spectra scattered from liquid H_2O and D_2O samples, a series of phenomena with relation to the complicated motions of the molecules in these liquids have been elucidated. Particularly it has again been shown that the cold neutron technique offers a good tool to study phenomena occurring on a time scale with a unit of 10^{-13} sec. The following facts have been observed and conclusions drawn:

Par. 1. The angular variation of the elasticly scattered intensity is determined by a factor $e^{-0.142\,\kappa^2}$, which corresponds to a Debye temperature of 130 ^{o}K.

Par. 2. The elasticly scattered spectrum shows a line broadening corresponding to a natural line width of $6 \cdot 10^{-4}$ eV. In accordance to other theoretical work this might mean that the molecules on the average oscillate for a time at $2 \cdot 10^{-12}$ sec before they make a diffusion jump of at least 1.5 Å length.

Par. 3. When the sample temperature is elevated the line width increases much less than predicted by a continuous diffusion model.

Par. 4. The temperature variation of the elasticly scattered intensity as observed at a particular angle, 30^{o}, is in agreement with the predictions of both models.

Par. 5. The inelasticly scattered spectrum shows two peaks corresponding to energy transfers of 0.059 and 0.020 eV in H_2O and 0.048 and 0.016 eV in D_2O which might be of the nature already proposed by Raman spectroscopy: one hindered rotation and a particular type of vibration, respectively.

Par. 6. The inelasticly scattered spectrum also shows a part corresponding to energy transitions from 0.010 eV and down to zero in H_2O as well as in D_2O, which for H_2O shows an angular variation in agreement with a calculations, based

on the solid-like structure of water. This observation also is in agreement with the Debye-temperature determined from the elasticly scattered spectra.

Par. 7. The gas model (M = 18) for the molecular motion does not lead to cross section values in agreement with observation.

Par. 8. Except for the pronounced coherence effects in the scattering from D_2O, light and heavy water show the same general type of scattered spectra, indicating the very close relationship between the dynamical behaviour of the two liquids.

The measurements thus show that studied on a time scale with a unit of 10^{-13} seconds, water - light and heavy - shows properties very similar to those of a solid. On the basis of this experiment it is to be expected that the properties would appear fluid-like, for observation times much larger than 10^{-12} seconds.

References.

1. van HOVE L
Phys. Rev. 95, 249 (1954)

2. CARTER R S, PALEVSKY H and HUGHES D J
Phys. Rev. 106, 1168 (1957)

BROCKHOUSE B N and STEWART A T
Rev. Mod. Phys. 30, 236 (1959)

3. STEWART A T and BROCKHOUSE B N
Rev. Mod. Phys. 30, 250 (1958)

EISENHAUER C M, PELAH I, HUGHES D J and PALEVSKY H
Phys. Rev. 109, 1046 (1958).

4. LARSSON K E, DAHLBORG U and HOLMRYD S
Arkiv f. Fysik, 17, 369 (1960).

5. BROCKHOUSE B N
N. 1 del Supplemento al Vol. 9, Serie X del Nuovo Cimento, 45 (1958)

6. BROCKHOUSE B N
Phys. Rev. Letters 2, 287 (1959).

7. HUGHES D J, PALEVSKY H, KLEIN W and TUNKELO E
Phys. Rev. Letters 3, 91 (1959)

8. SINGWI K S and SJÖLANDER A
Bull. Am. Phys. Soc. 5, 168 (1959)

9. LARSSON K E, DAHLBORG U, HOLMRYD S, OTNES K and STEDMAN R
Arkiv f. Fysik 16, 199 (1959)

10. LARSSON K E, STEDMAN R and PALEVSKY H
JNE 6, 222 (1958)

11. VINEYARD GEORGE H
Phys. Rev. 110, 999 (1958)

12. SIMPSON J H and CARR H Y
Phys. Rev. 111, 1201 (1958).

13. SJÖLANDER ALF
Arkiv f. Fysik 14, 315 (1958)

14. PELAH, EISENHOWER, HUGHES and PALEVSKY
Phys. Rev. 108, 1091 (1957)

ANDRESEN, Mc REYNOLDS, NELKIN, ROSENBLUTH and WHITTEMORE
Phys. Rev. 108, 1092 (1957)

15. BERGSMA J
Unpublished results on different hydrides. Work made at RI in Stockholm

16. MAGAT M
Ann. de Physique, 6, 108 (1936)

17. CROSS PAUL C, BURNHAM JOHN and LEIGHTON PHILIP A
Journ. Amer. Chem. Soc. 59, 1134 (1937)

18. NELKIN MARK
General Atomic Report GA-1063 (1960)

19. KRIEGER T J and NELKIN M S
Phys. Rev. 106, 290 (1957)

Figure Captions

Figure 1. Neutron spectra scattered at angles of observation between 30° and 122°. Sample thickness = 1.4 mm.

Figure 2. Neutron spectra scattered at an angle of observation of 30° for sample thickness in the range from 5 down to 0.2 mm.

Figure 3. The ratio between the intensities observed at 900 μsec ~ 1 Å to those observed at 3200 μsec ~ 4 Å for the different sample thicknesses.

Figure 4. Thin sample (0.2 mm) observations at the angles of 30° and 90°.

Figure 5. Separation of the observed spectra into one inelasticly scattered part represented by curves I, II and III and one quasi-elastic represented by curve IV.

Figure 6. Elasticly scattered neutron spectra (curves IV of figure 5) compared to the primary cold neutron spectrum.

Figure 7. Observed broadening of the sharp beryllium cut off at 3.96 Å as a function of the momentum transfer, κ. Given are also the line widths predicted by the continuous diffusion model (Vineyard) and by the quasi-crystalline model (Singwi - Sjölander).

Figure 8. Intensity variation of the quasi-elasticly scattered peak as a function of momentum transfer, $\kappa = \frac{4\pi}{\lambda_o} \sin\frac{\varphi}{2}$.

Figure 9. The change of shape of the spectrum scattered at $\varphi = 30^{\circ}$ as a function of sample temperature.

Figure 10. The variation of the width of the quasi-elasticly scattered beryllium cut off as a function of sample temperature. Given is also the broadening expected on the basis of the continuous diffusion model.

Figure 11. The quasi-elasticly scattered intensity as a function of temperature at an angle of observation of $\varphi = 30^{\circ}$.

Figure 12. Observed "acoustic vibrational" spectrum compared to calculated Debye spectra at the angles of observation of 30° and 90°.

Figure 13. Various gas model spectra (M = 18 and M = 100) compared to the appropriate part of the experimentally observed spectrum at an angle of 90°.

Figure 14. Angular distribution of elasticly scattered neutrons from a 2 mm D_2O sample. Neutron wave length = 1.1 A.

Figure 15. Elasticly and inelasticly scattered spectra from D_2O for angles of observation of 30° and 90°. Sample thickness = = 2 mm.

KEL, SH, KO/EL

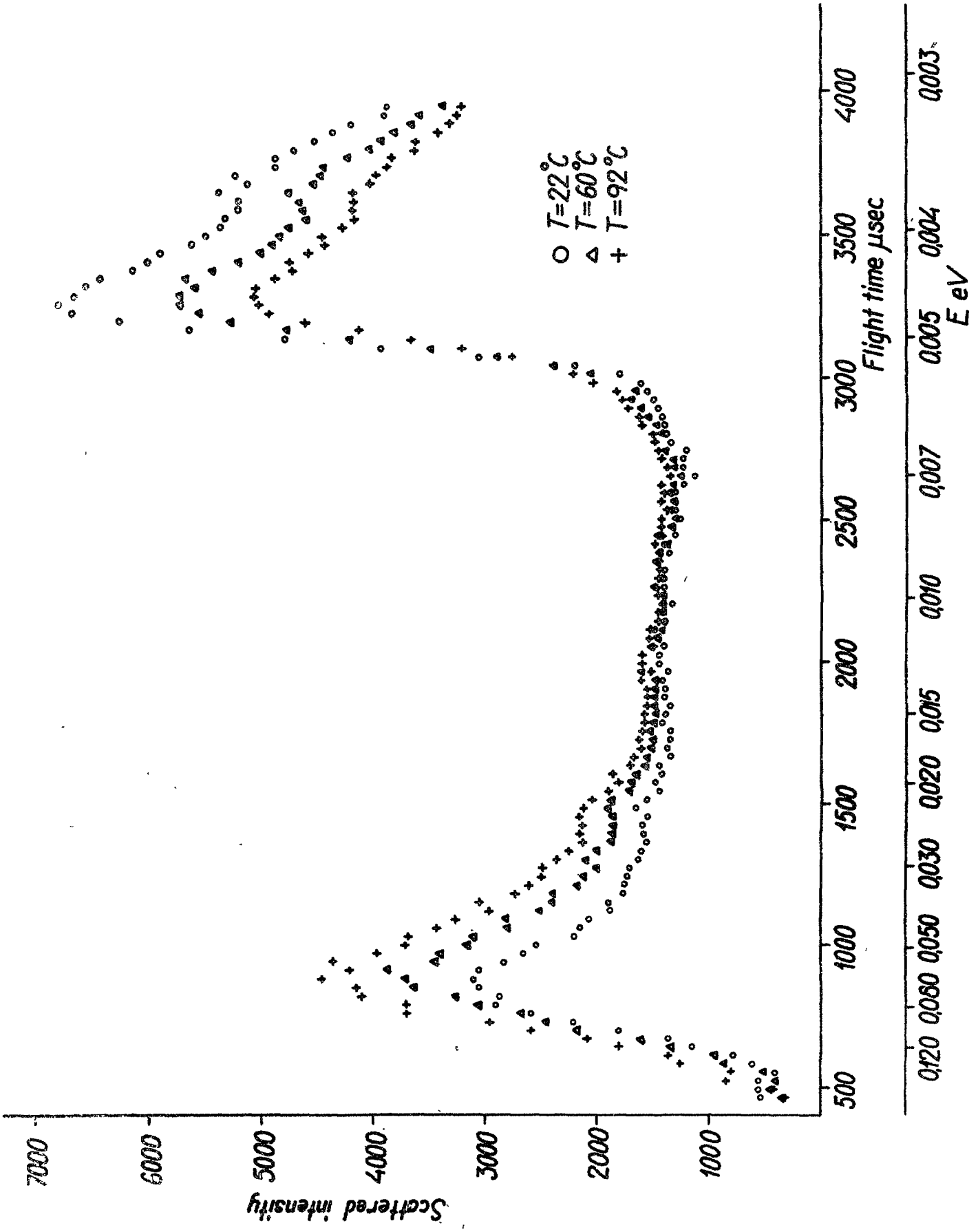

Figure 1. Neutron spectra scattered at angles of observation between 30° and 122°. Sample thickness = 1,4 mm.

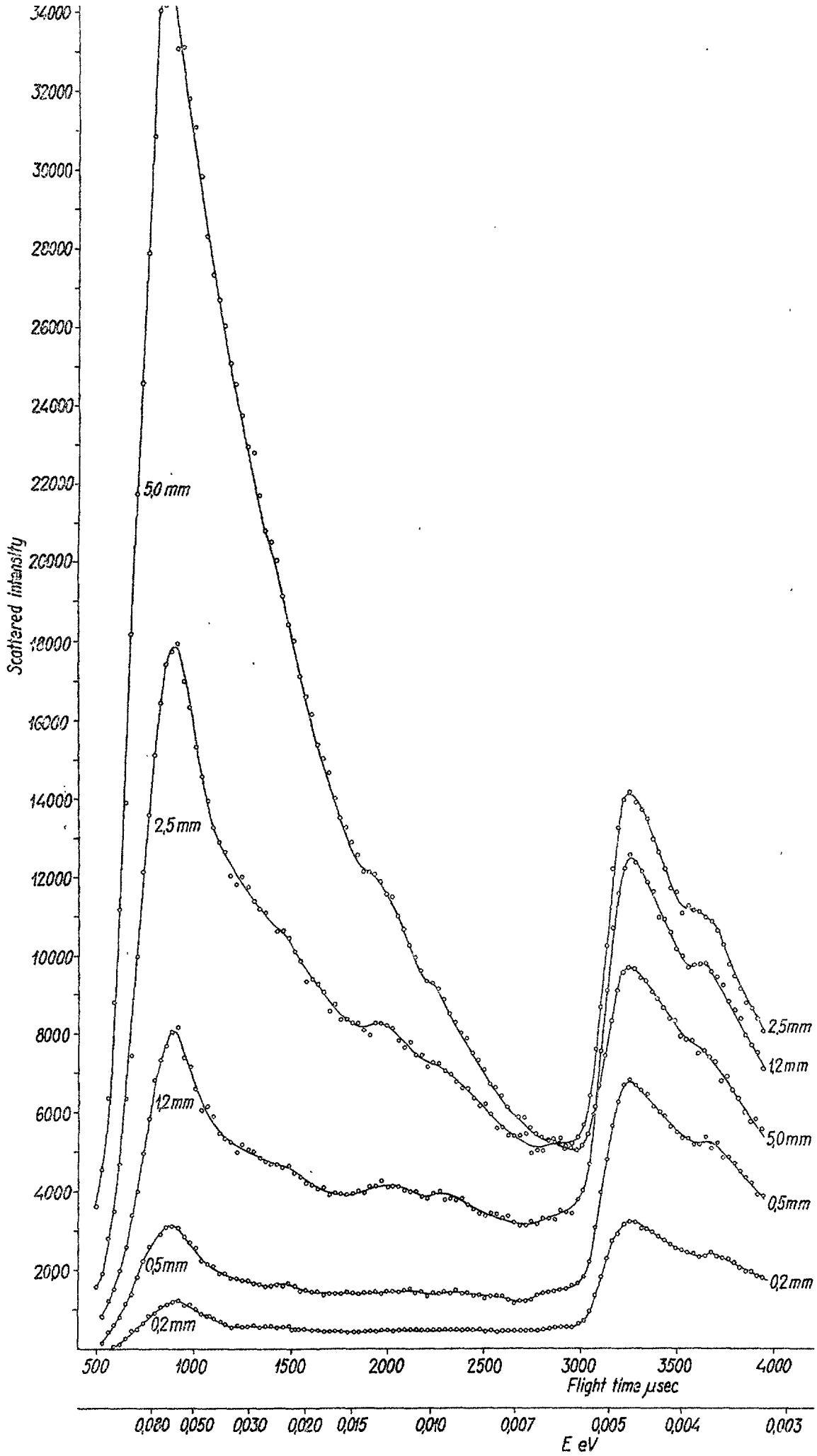

Figure 2. Neutron spectra scattered at an angle of observation of 30° for sample thickness in the range from 5 down to 0.2 mm.

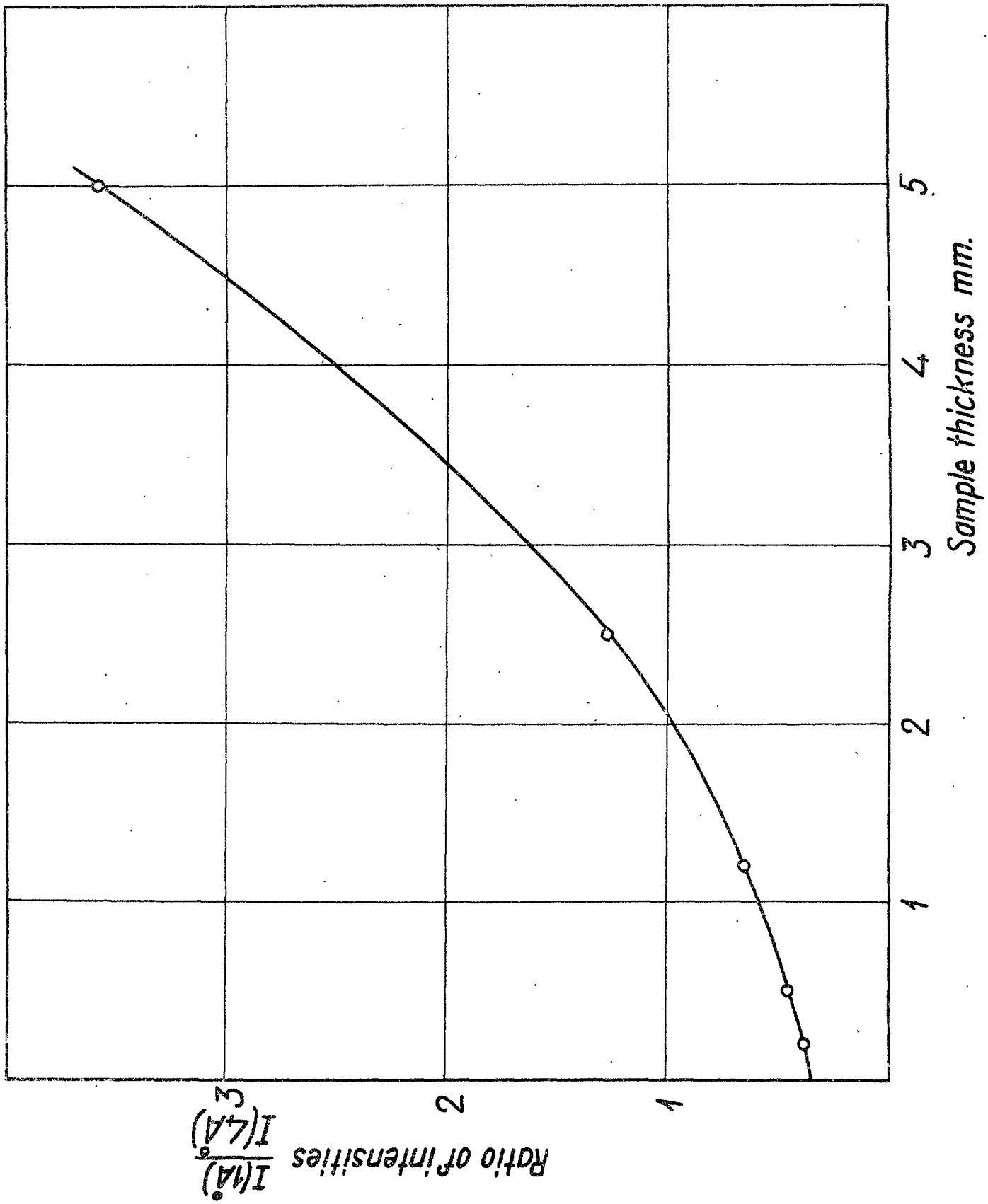

Figure 3. The ratio between the intensities observed at 900 μsec ~ 1 Å to those observed at 3200 μsec ~ 4 Å for the different sample thicknesses.

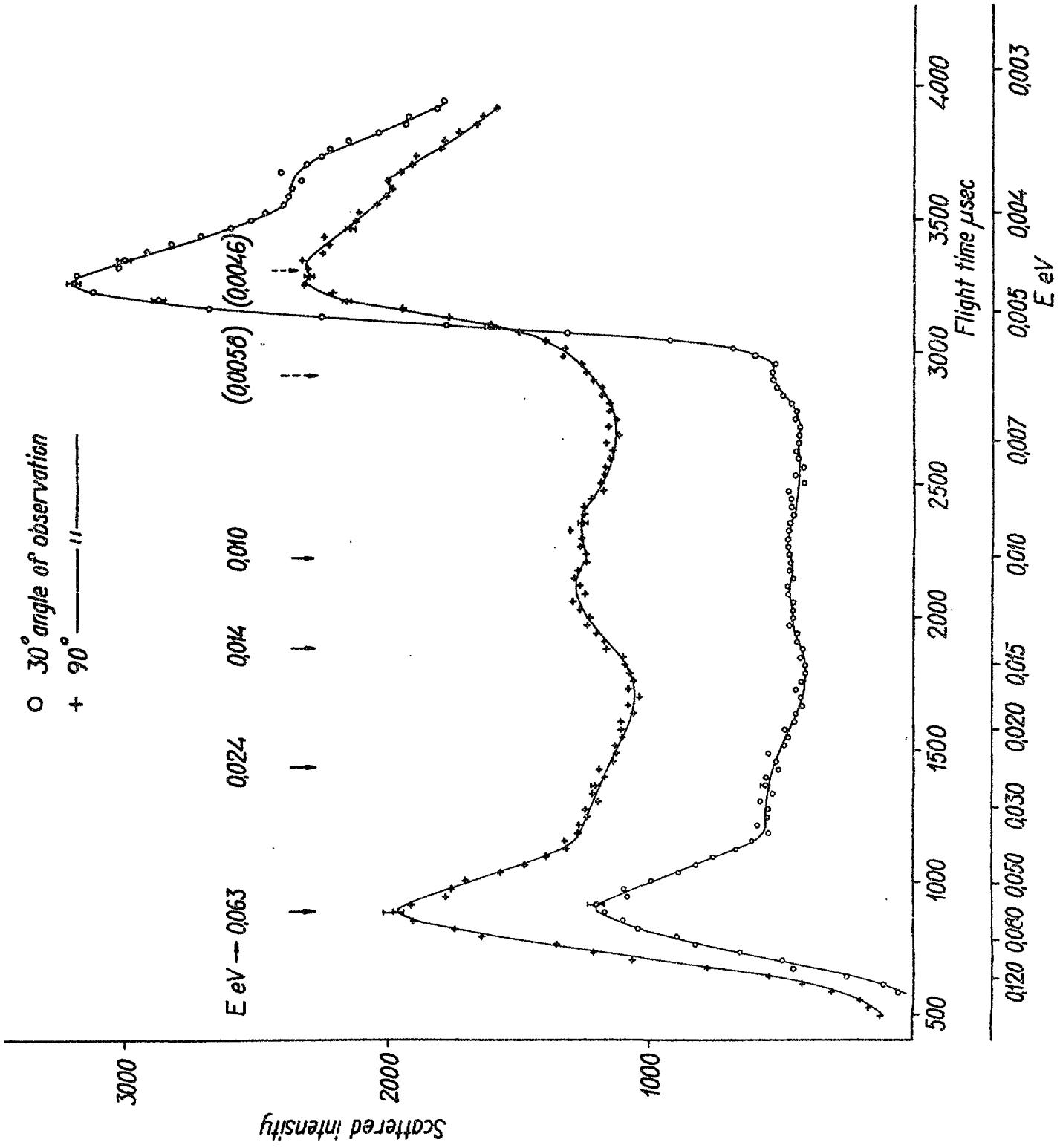

Figure 4. Thin sample (0.2 mm) observations at the angles of 30° and 90°.

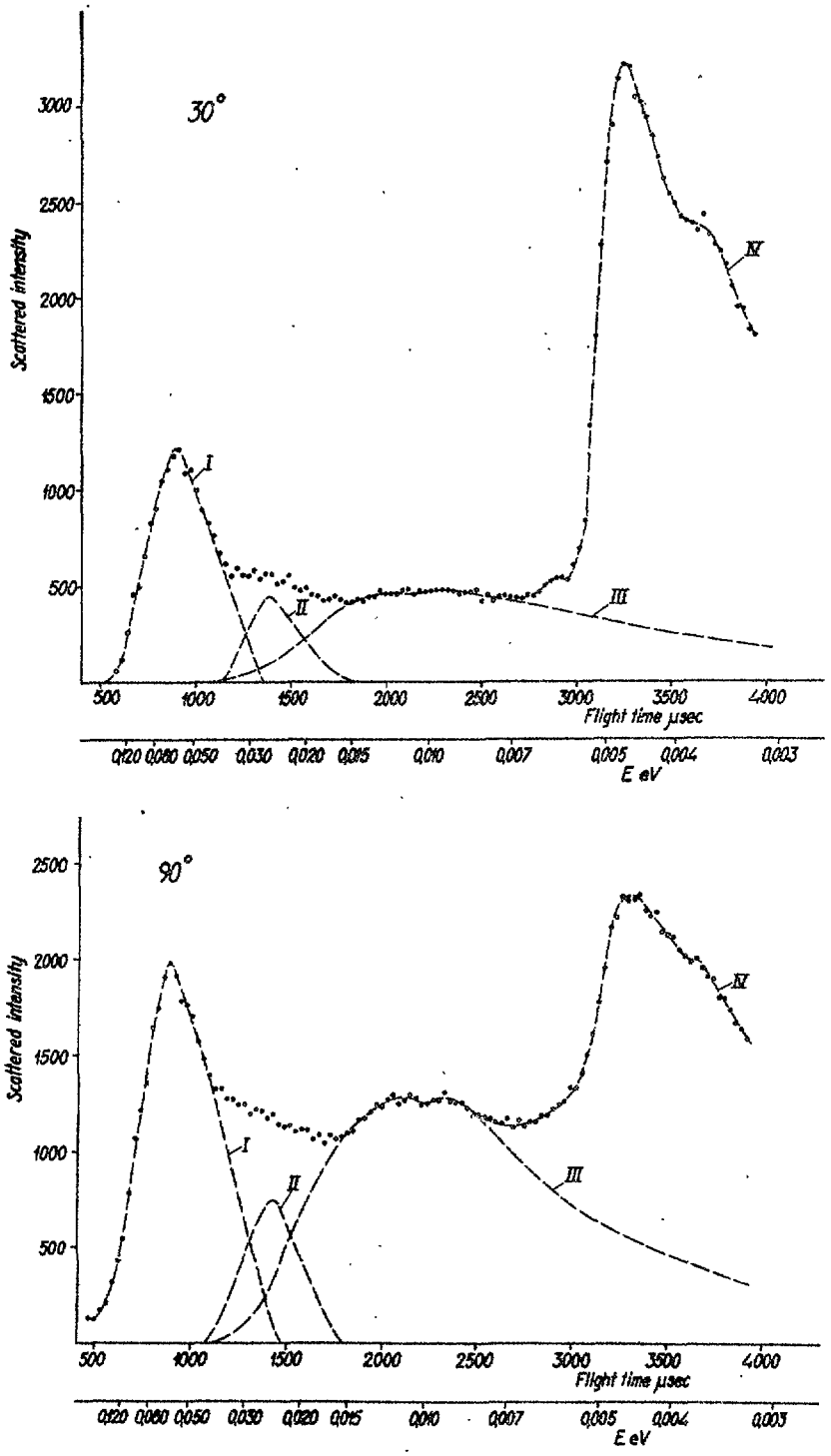

Figure 5. Separation of the observed spectra into one inelasticly scattered part represented by curve I, II and III and quasi-elastic represented by curve IV.

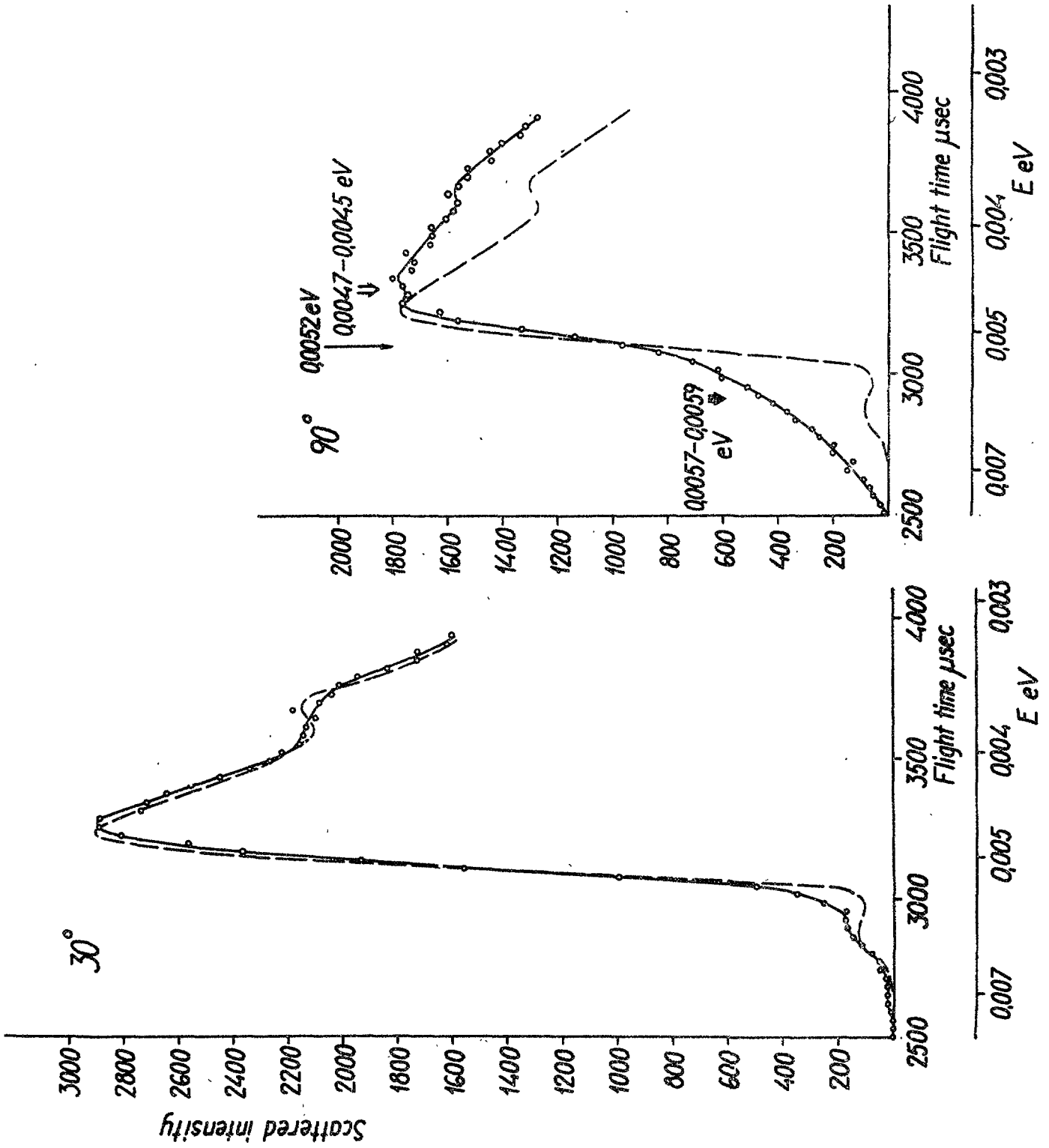

Figure 6. Elasticly scattered neutron spectra (curved IV of figure 5) compared to the primary cold neutron spectrum.

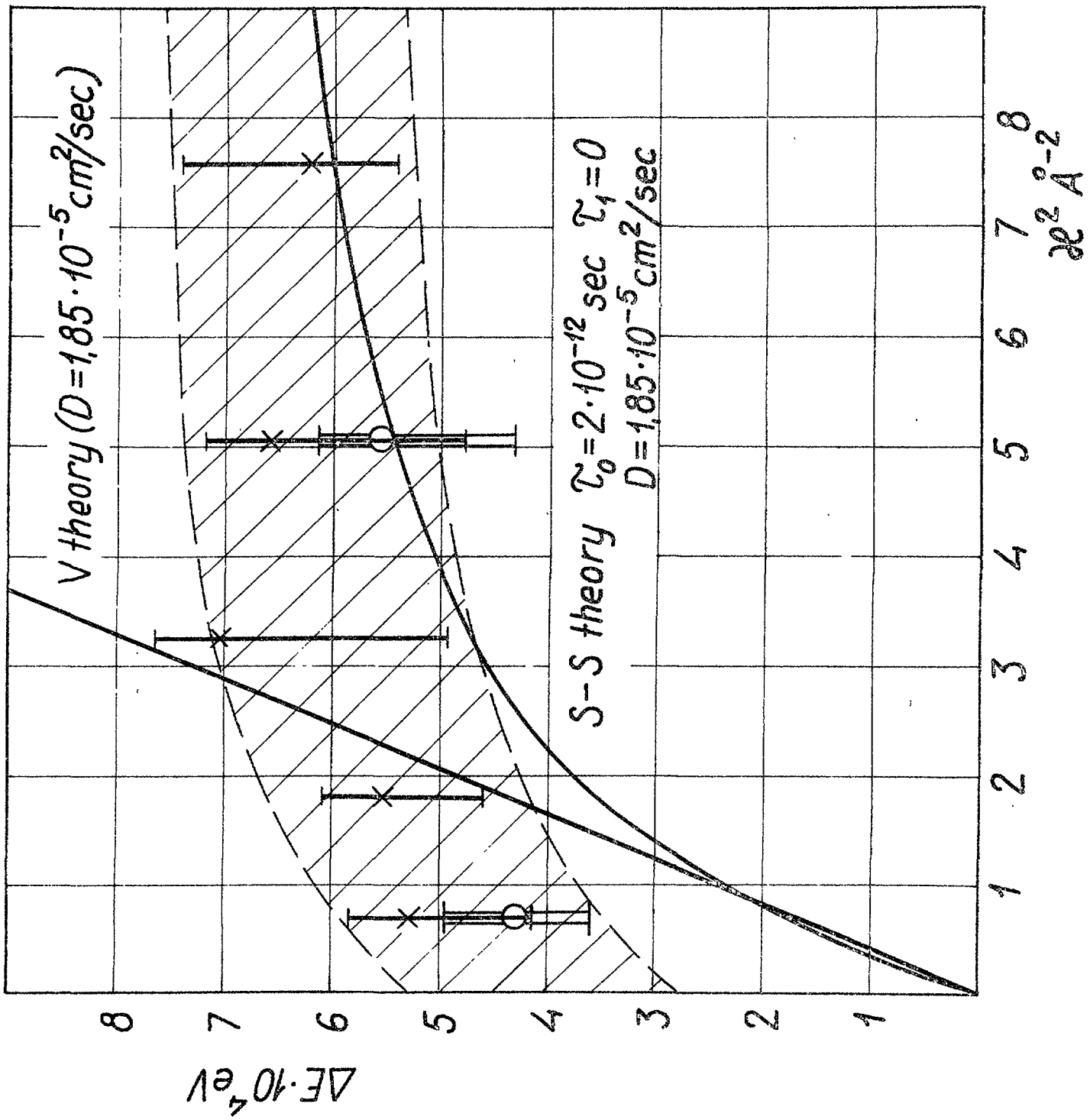

Figure 7. Observed broadening of the sharp beryllium cut off at 3.96 A as a function of the momentum transfer, κ. Given are also the line widths predicted by the continuous diffusion model (Vineyard) and by the quasi-crystalline model (Singwi-Sjölander).

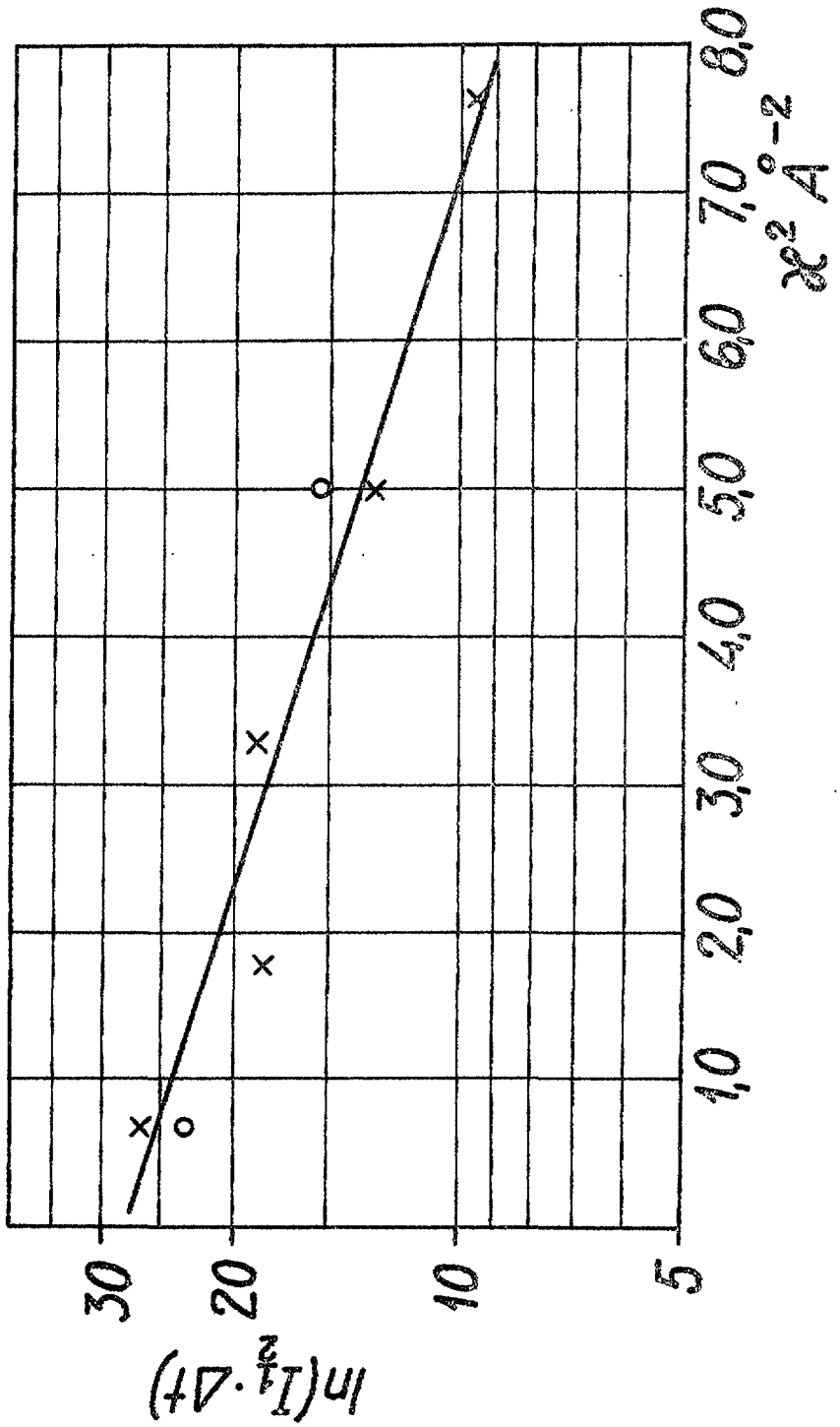

Figure 8. Intensity variation of the quasi-elasticly scattered peak as a function of momentum transfer $\varkappa = \frac{4\pi}{\lambda_0} \sin \frac{\varphi}{2}$.

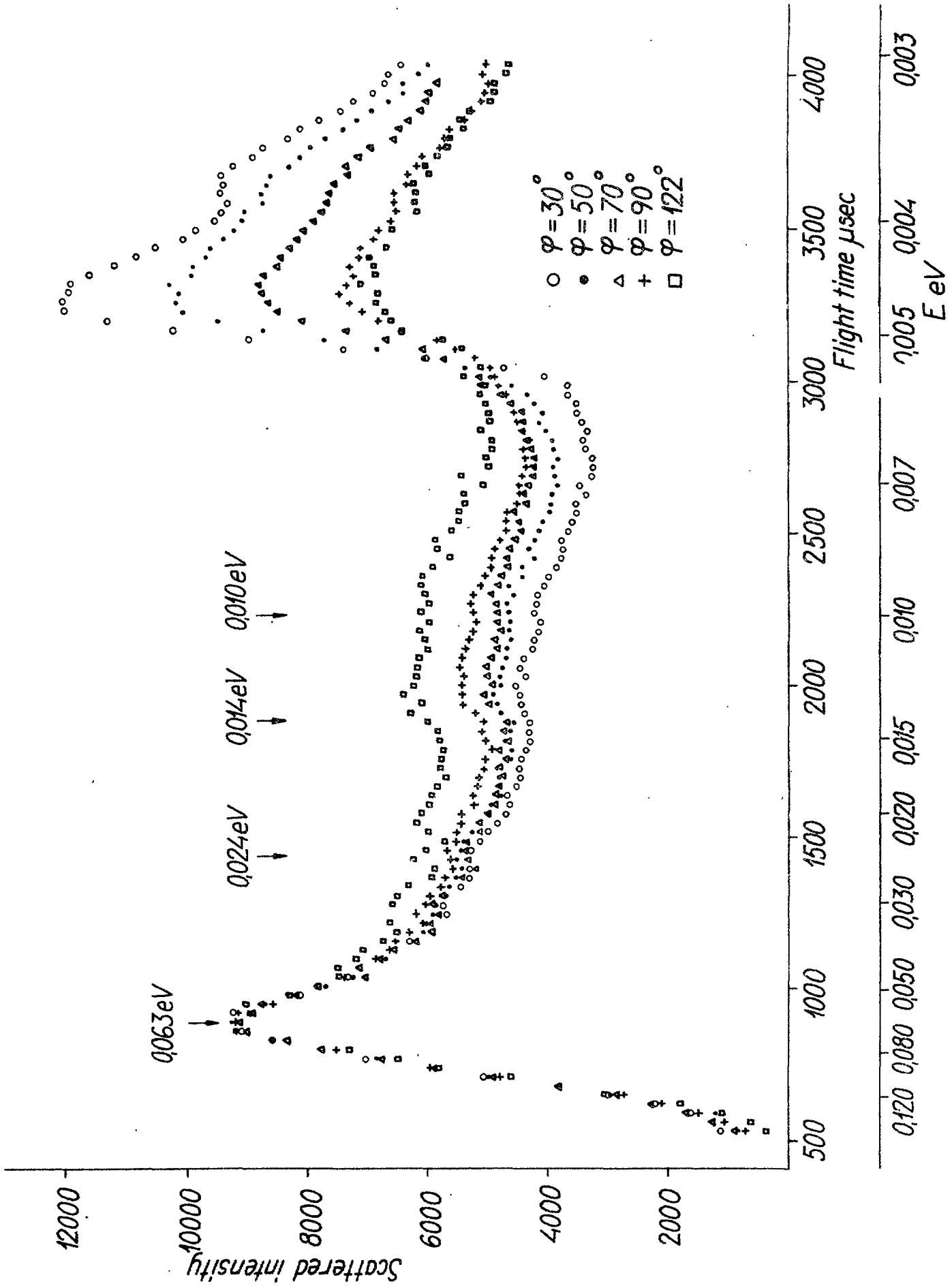

Figure 9. The change of shape of the spectrum scattered at $\varphi = 30^{\circ}$ as a function of sample temperature.

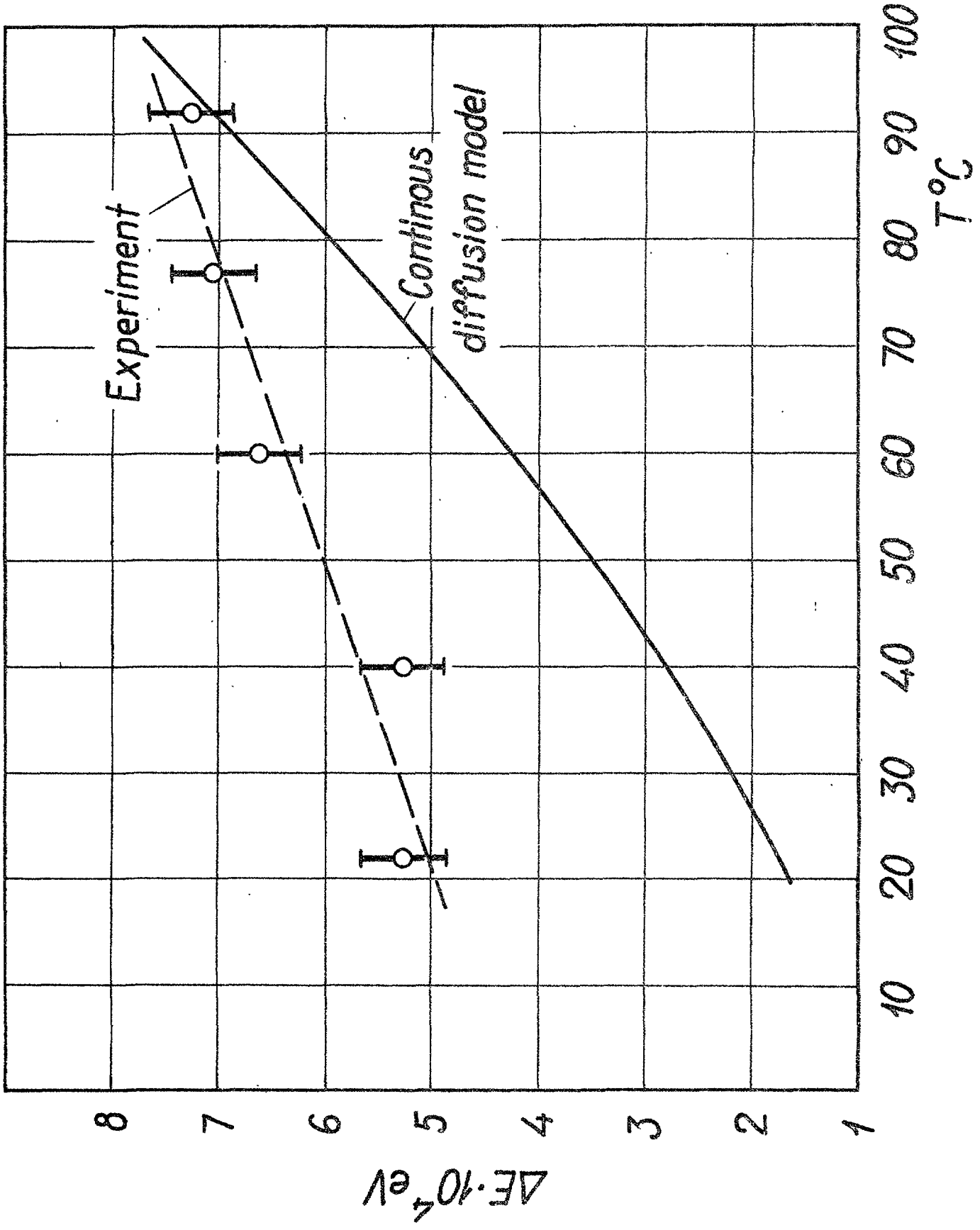

Figure 10. The variation of the width of the quasi-elasticly scattered beryllium cut off as a function of sample temperature. Given is also the broadening expected on the basis of the continuous diffusion model.

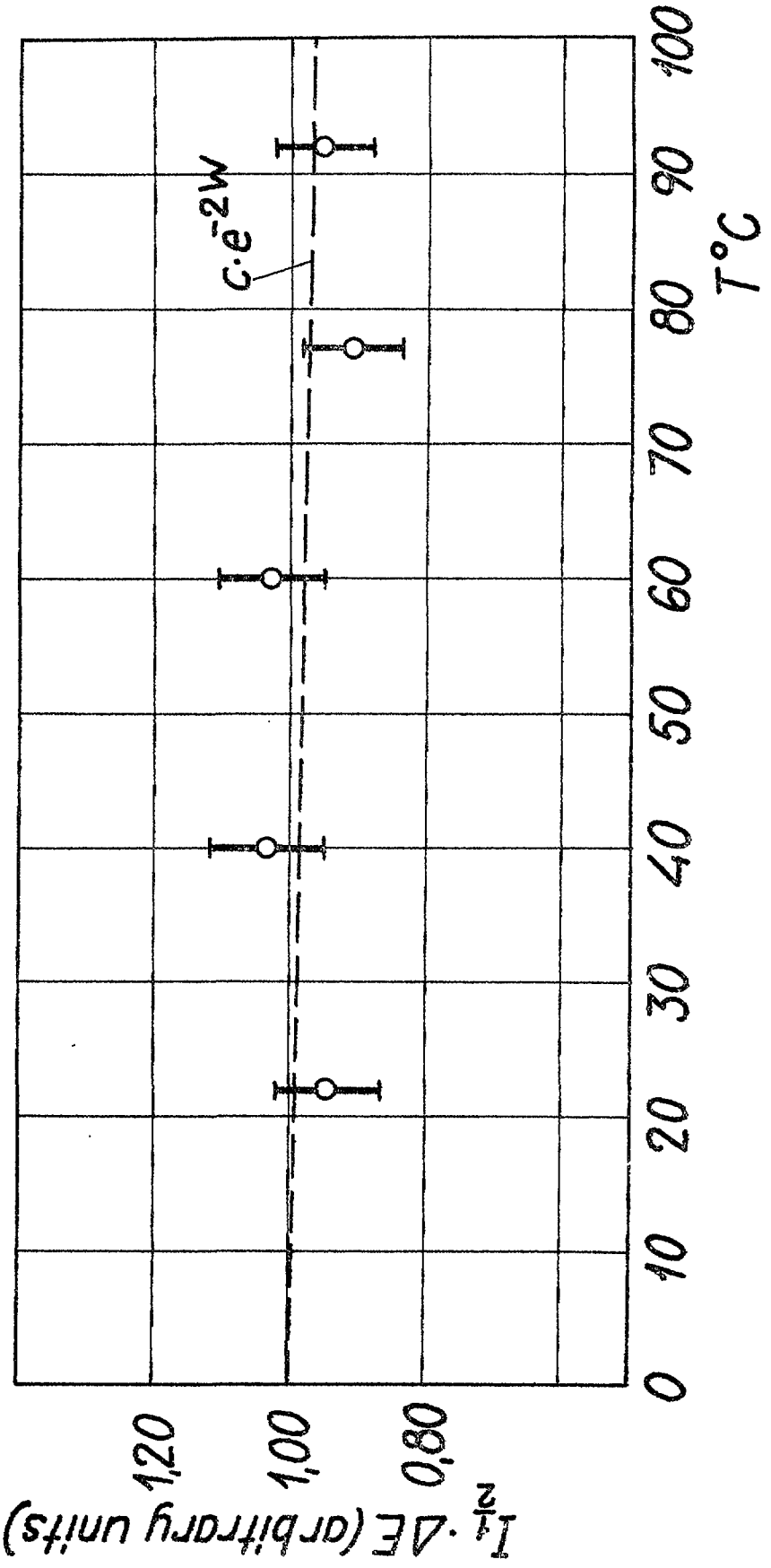

Figure 11. The quasi-elasticly scattered intensity as a function of temperature at an angle of observation of $\varphi = 30^{\circ}$.

LIST OF AVAILABLE AE-REPORTS

Additional copies available at the library of
AB ATOMENERGI
Stockholm - Sweden

AE No	Title	Author	Printed in	Pages	Price in Sw. cr.
1	Calculation of the geometric buckling for reactors of various shapes	*N. G. Sjostrand*	1958	23	3
2	The variation of the reactivity with the number, diameter and length of the control rods in a heavy water natural uranium reactor.	*H McCrirrick*	1958	24	3
3	Comparison of filter papers and an electrostatic precipitator for measurements on radioactive aerosols	*R Wiener*	1958	4	4
4	A slowing-down problem.	*I. Carlvik, B. Pershagen*	1958	14	3
5	Absolute measurements with a 4π-counter. (2nd rev. ed.)	*Kerstin Martinsson*	1958	20	4
6	Monte Carlo calculations of neutron thermalization in a heterogeneous system.	*T. Hogberg*	1959	13	4
8	Metallurgical viewpoints on the brittleness of beryllium	*G. Lagerberg*	1960	14	4
9	Swedish research on aluminium reactor technology.	*B. Forsén*	1960	13	4
10	Equipment for thermal neutron flux measurements in Reactor R2.	*E. Johansson, T. Nilsson, S. Claesson*	1960	9	6
11	Cross sections and neutron yields for U^{233}, U^{235} and Pu^{239} at 2200 m/sec	*N. G. Sjostrand J S Story*	1960	34	4
12	Geometric buckling measurements using the pulsed neutron source method	*N. G Sjostrand, J Mednis, T. Nilsson*	1959	12	4
13	Absorption and flux density measurements in an iron plug in R1	*R. Nilsson, J. Braun*	1958	24	4
14	GARLIC, a shielding program for GAmma Radiation from LIne- and Cylinder-sources.	*M. Roos*	1959	36	4
15	On the spherical harmonic expansion of the neutron angular distribution function.	*S Depken*	1959	53	4
16	The Dancoff correction in various geometries.	*I. Carlvik, B Pershagen*	1959	23	4
17	Radioactive nuclides formed by irradiation of the natural elements with thermal neutrons.	*K Ekberg*	1959	29	4
18	The resonance integral of gold	*K Jirlow, E. Johansson*	1959	19	4
19	Sources of gamma radiation in a reactor core.	*M. Roos*	1959	21	4
20	Optimisation of gas-cooled reactors with the aid of mathematical computers.	*P. H. Margen*	1959	33	4
21	The fast fission effect in a cylindrical fuel element.	*I. Carlvik, B. Pershagen*	1959	25	4
22	The temperature coefficient of the resonance integral for uranium metal and oxide.	*P. Blomberg, E. Hellstrand, S. Horner*	1960	25	4
23	Definition of the diffusion constant in one-group theory	*N. G. Sjostrand*	1960	8	4
25	A study of some temperature effects on the phonons in aluminum by use of cold neutrons.	*K-E Larsson, U Dahlborg, S. Holmryd*	1960	32	4
26	The effect of a diagonal control rod in a cylindrical reactor	*T. Nilsson, N. G. Sjöstrand*	1960	4	4
28	RESEARCH ADMINISTRATION: A selected and annotated bibliography of recent literature	*E Rhenman, S Svensson*	1960	49	6
29	Some general requirements for irradiation experiments.	*H. P. Myers, R. Skjoldebrand*	1960	9	6
30	Metallographic Study of the Isothermal Transformation of Beta Phase in Zircaloy-2.	*G. Östberg*	1960	47	6
32	Structure investigations of some beryllium materials	*I. Fäldt, G. Lagerberg*	1960	15	6
33	An Emergency Dosimeter for Neutrons.	*J. Braun, R. Nilsson*	1960	32	6
35	The Multigroup Neutron Diffusion Equations /1 Space Dimension	*S. Linde*	1960	41	6

Affärstryck, Stockholm 1960